Characterization of the Secondary Structure and Stability of an RNA Aptamer That Binds Vascular Endothelial Growth Factor†

Melanie Bozza,‡ Richard D. Sheardy,*,‡ Enrique Dilone,§ Stephen Scypinski,§ and Margaret Galazka§

Department of Chemistry and Biochemistry, Seton Hall University, South Orange, New Jersey 07079, and Eyetech Pharmaceuticals, Inc., Morris Plains, New Jersey 07927

Received October 20, 2005; Revised Manuscript Received February 16, 2006

ABSTRACT: Thermal denaturation studies and spectroscopic studies were employed to investigate the secondary structure and stability of an RNA−PEG conjugate commercially called Macugen. The RNA aptamer is conjugated to a pegylated moiety, and the majority of its 2′-hydroxyl groups are methylated or otherwise modified. UV optical melting studies and differential scanning calorimetry (DSC) were carried out under different conditions to evaluate the effects of Na^+ and oligomer concentrations on the stability of the secondary structure of the RNA oligomer. The results of these studies indicated that the T_m of the RNA is independent of oligomer concentration but dependent on the salt concentration, in a predictable fashion. Further, the DSC melting profiles obtained under all conditions were highly reversible. Circular dichroism (CD) studies were determined under different salt concentrations, various RNA concentrations, and temperatures as well. Together, the thermal denaturation and CD studies provide evidence that the secondary structure of the RNA oligonucleotide is a stable hairpin at 25 °C and that the thermally induced hairpin to single strand transition is highly reversible.

The human genome project collects nucleic acid sequence data and provides a foundation for rapidly generating new databases of RNA secondary structures (*1*−*4*). RNA secondary structures are important for understanding structure−function relationships, choosing drug targets or drugs themselves which target other biological structures. RNA can occur as a single polynucleotide chain, but many exist in elaborate defined secondary structures containing short double helical regions connected by single-stranded stretches such as loops or bulges. Helical hairpin regions can be formed due to the antiparallel orientation of some complementary sequences found in different regions of the RNA chain. Although most of these double helical regions contain standard A·U and C·G base pairs, they may also contain a number of energetically less stable G·U base pairs. These non-Watson−Crick hydrogen-bonding interactions have been shown to stabilize loops and bulges in single-stranded regions of RNA (*5*−*9*).

RNA aptamers are synthetic polymers that are selected from random sequence libraries and optimized for their ability to bind to a specific target molecule. Systematic evolution of ligands by exponential enrichment (SELEX) has led to the development of aptamer sequences with many desired binding properties. These aptamers are being used in place of antibiotics and show promise as clinical diagnostic tools as well as for drug therapies. Development of aptamers has been long overdue since native nucleic acids are typically poorly suited for use as drugs. RNA degrades readily under in vitro conditions while DNA is more stable (*10*). The development of stable RNA derivatives, such as Macugen, has created a whole new library of potential therapeutics. This drug is currently on the market for the treatment of age-related macular degeneration. Its mode of action is via binding to VEGF (vascular elongation growth factor), resulting in the inhibition of the growth of new blood vessels. Macugen is a 27 base RNA oligonucleotide possessing 2′-*O*-methyl and 2′-*O*-fluoro modifications conjugated to poly(ethylene glycol) (PEG). The 2′-*O*-methyl and 2′-*O*-fluoro modifications stabilize the RNA by precluding phosphate hydrolysis but do not apparently affect the stability of the secondary structure of the aptamer itself (*11*). The PEG modification helps to stabilize the RNA in solution and also facilitates clinical delivery. The 3′ terminus of the RNA is protected from exonuclease activity by the 3′−3′ linkage to dT. The sequence of the RNA conjugate is revealed in Scheme 1.

We report here structural and thermodynamic studies on this modified RNA conjugate. The results indicate that the RNA portion of the conjugate assumes a hairpin conformation designated as the aptamer. Maintenance of the aptamer's structure is dependent on environmental conditions such as salt concentration, pH, temperature, and the presence of ions. The major sequence-dependent forces that drive the helix formation, such as base stacking and hydrogen bonding, are affected by these environmental conditions.

MATERIALS AND METHODS

Materials. Eyetech Pharmaceuticals, Inc., generously provided the RNA−PEG conjugate Macugen. All solid buffer components were purchased from Sigma Chemicals

† This project was generously supported by Eyetech Pharmaceuticals, Inc.

* Address correspondence to this author: (973) 761-9030 (phone); (973) 761-9772 (fax); sheardri@shu.edu (e-mail).

‡ Seton Hall University.

§ Eyetech Pharmaceuticals, Inc.

10.1021/bi0521442 CCC: $33.50 © 2006 American Chemical Society
Published on Web 05/19/2006

Scheme 1: Primary Sequence of the RNA−PEG (Macugen) Conjugate[a]

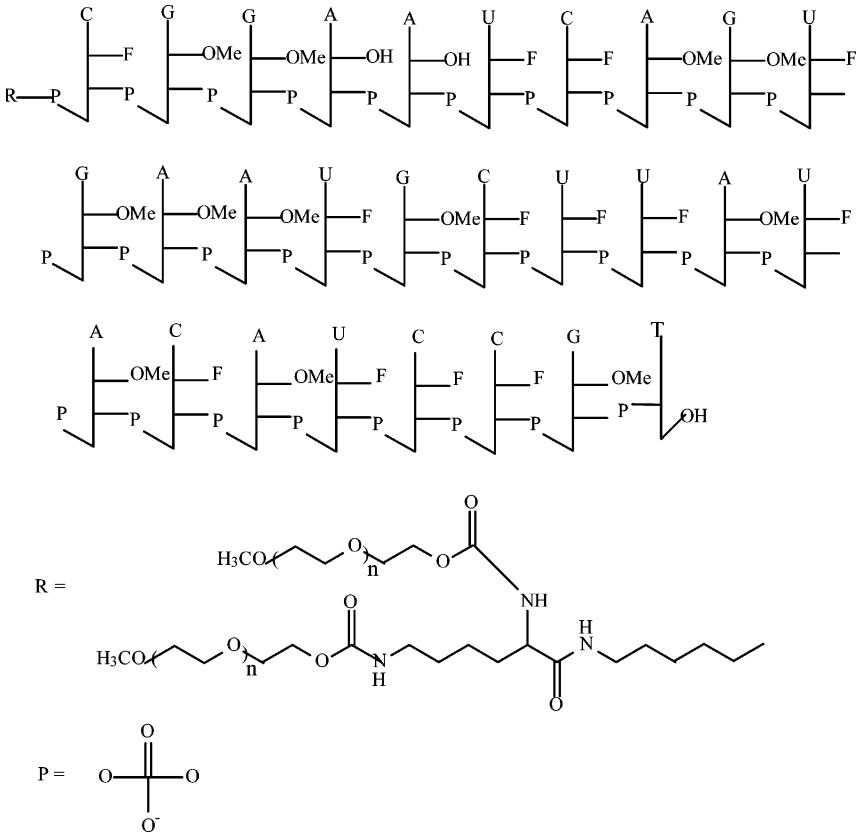

[a] This is a 27 base RNA oligonucleotide possessing 2′-flourocytidine, 2′-flourouridine, 2′-methoxyadenosine, 2′-methoxyguanosine, and unmodified adenosine. The RNA oligonucleotide is conjugated at the 3′ terminus to poly(ethylene glycol) (PEG), where *n* is about 450. A terminal thymidine is linked to the RNA chain via a 3′−3′ linkage.

or Fisher Scientific and were used without further purification. The water used for the buffer solutions was deionized, twice distilled, and then sterilized. The RNA−PEG conjugate was prepared in standard phosphate buffer (5 mM NaH_2PO_4, 5 mM Na_2HPO_4, 0.1 mM EDTA, pH 7.0) to final concentrations of RNA between 0.008 and 0.8 mg/mL and of Na^+ from 50 mM to 1 M. The aptamer concentration for each sample was determined by spectrophotometric absorbance, using an extinction coefficient of 27 mL cm^{-1} (mg of RNA)$^{-1}$ as provided by the supplier.

Circular Dichroism Spectropolarimetry (CD). Circular dichroism spectra were recorded at 25 or 37 °C with an Aviv Associates CD spectropolarimeter, model 62-ADS, equipped with a multiple cell turret, Peltier heating/cooling device, and nitrogen purging capabilities. Prior to all CD measurements the samples were transferred from 2−5 °C storage and thermally equilibrated in stoppered cuvettes for 15−20 min. The CD spectrum of the RNA aptamer was recorded from 320 to 220 nm; the data were the average of triplicate scans. All spectral data were blank-corrected and processed with Aviv DOS-based software for subsequent export into graph-plotting software.

Differential Scanning Calorimeter (DSC). All heat capacity measurements were made with a Nano-II power-compensation differential scanning calorimeter from Calorimetric Sciences Corp. The calorimeter was interfaced directly to a Windows-based computer with "DSCRun" version 2.1.1 software (Calorimetric Sciences Corp.) for both data collection and DSC control. The reference solution for the reference side of the calorimetric measurement was derived from the buffer used to equilibrate the sample. Calorimetric measurements were performed as the average of two independent samples. Each RNA aptamer sample was thermally scanned from 20 to 95 °C at 0.5 °C/min over a minimum of four forward and four reverse scans. The samples were equilibrated for 10 min at the upper (reverse scan) or lower (forward scan) set points between thermal scans. The raw thermographic data were blank-corrected and integrated with "CpCalc" version 2.1 (Calorimetric Sciences Corp.) software. For most samples, the nature of the pretransition and posttransition baselines enabled integration of the calorimetric enthalpy with the use of a linear baseline.

UV−Visible Spectroscopy. Either a Cary model 300E Bio or Cary model 100E spectrophotometer from Varian, Inc., was used for all UV−vis spectral measurements. Both instruments were interfaced to Windows-based computers with Cary/Varian WinUVBio version 2.0 software and equipped with a Peltier thermoelectric heating/cooling block, a multicell-transport device, and a sample compartment with nitrogen purge capability.

Thermal scanning of the aptamer was determined at the wavelength of maximum absorbance difference between the native form at 20 °C and the denatured form at 95 °C. Aptamer solutions with concentrations of RNA ranging from 0.008 to 0.80 mg/mL in standard phosphate buffer at 110 mM total Na^+ were equilibrated at 4 °C for 12−24 h prior to measurement. After equilibration the aptamer solutions were transferred to cuvettes equilibrated at the experimentally relevant start temperature and equilibrated for an additional 20 min. Typically, the aptamer samples were "ramped" from

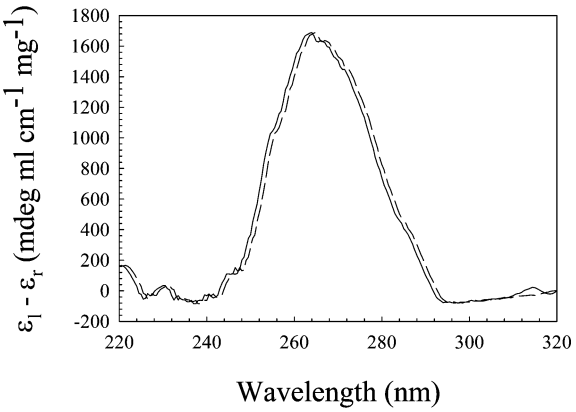

FIGURE 1: CD spectra of the RNA aptamer at 25 °C (solid line) and 37 °C (dashed line) in standard phosphate buffer at 110 mM Na^+ at a total RNA strand concentration of 0.08 mg/mL.

20 to 95 °C at approximately 0.3 °C/min with two forward and two reverse scans. The melting point values (T_m) for all RNA sequences were determined with Varian Cary "thermal" software, version 2.0, using a hyperchromicity model to fit the UV-melt data set to a self-complementary model with $n = 1$.

RESULTS AND DISCUSSION

Circular Dichroism Studies. Typical CD spectra of the aptamer at 25 and 37 °C are shown in Figure 1. Examinations of these spectra indicate that the secondary structure of the RNA aptamer at 37 °C (i.e., physiological temperature) is essentially the same as at 25 °C with a strong peak around 263 nm and a shallow trough around 238 nm. These spectra are quite similar to those reported for RNA hairpins possessing internal mismatches (*5*). Hence, the CD results of Figure 1 suggest that the RNA forms a hairpin secondary structure and the duplexed region of the hairpin is A-form (*6*).

UV−Visible Optical Melting Studies. To ascertain the hairpin structure for the RNA aptamer, optical melting studies were carried out. These studies monitor the thermally induced duplex to single strand transition by recording the absorbance of the sample at 260 nm as the temperature is slowly increased. The midpoint of the transition is called the T_M (i.e., melting temperature) and is an indirect measure of the thermodynamic stability of the duplexed regions of the hairpin. According to Marky and Breslauer (*12*), the melting temperature of a nucleic acid duplex is dependent upon the nucleic acid concentration for any transition with a molecularity greater than unity. However, for a unimolecular transition, such as the case for the hairpin to single strand transition, the T_M is independent of strand concentration. Hence, the T_m of the RNA hairpin was determined at aptamer RNA concentrations ranging from 0.008 to 0.80 mg/mL at 110 mM Na^+.

A typical melting curve is shown in Figure 2A. Above 45 °C, the melting curve has a sigmoidal shape indicative of a cooperative transition. In the range of 30−45 °C, there appears to be some complexity in the melt, suggesting deviation from two-state behavior. Nonetheless, at the temperature scan rates used for these studies (0.3 °C/min for both forward and reverse scans), there is no apparent hysteresis upon reannealing, indicating that the transition is

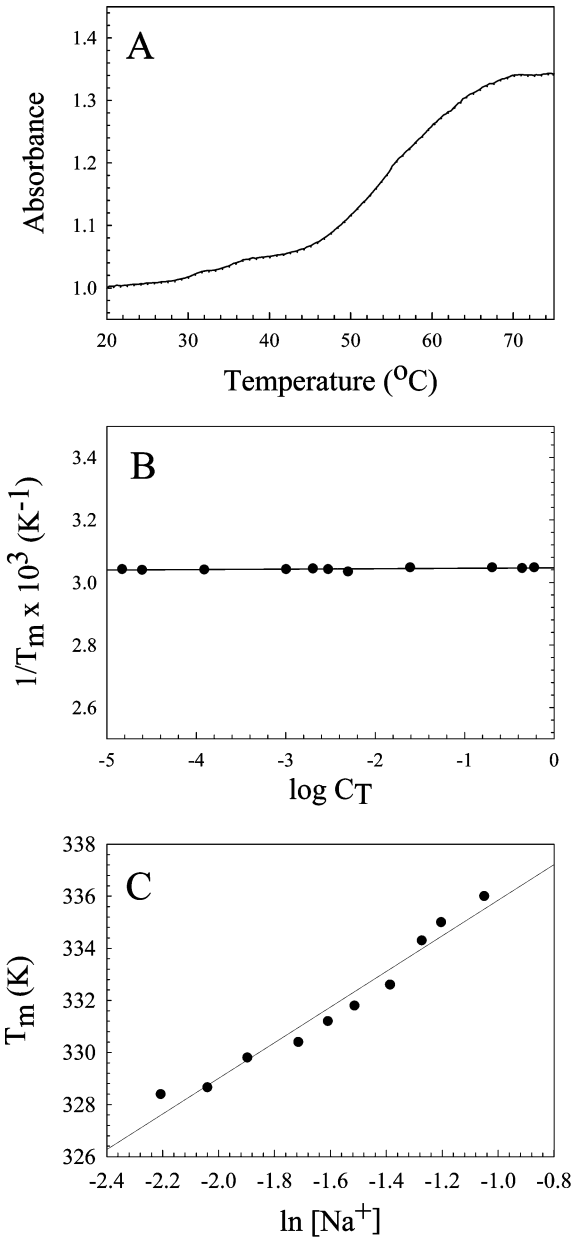

FIGURE 2: (A) Typical optical melting profile for the RNA (0.08 mg/mL) in standard phosphate buffer at 110 mM Na^+ at a heating rate of 0.3 °C/min (solid line) and a cooling rate of 0.3 °C/min (dotted line). (B) van't Hoff plot of $1/T_m$ vs log C_T (C_T is total strand concentration) for optical melts carried out in standard phosphate buffer at 110 mM Na^+ at a heating rate of 0.3 °C/min. (C) Plot of T_m vs natural log of the Na^+ concentration for the RNA at 0.08 mg/mL. For plots in panels B and C, the circles are the data points and the solid lines the least-squares linear fits.

fully reversible. Repeated denaturations of the same sample gave optical melting curves with a high degree of reproducibility (data not shown). Analysis of the data via the curve analysis program of the UV−vis spectrometer gave a van't Hoff enthalpy $\Delta H_{vH} = 387 \pm 25$ kJ/mol for the duplex to single strand transition. Construction of a van't Hoff plot of $1/T_m$ vs log C_T, where C_T is total strand concentration, yielded a linear plot with a near zero slope (Figure 2B). For all RNA concentrations studied, the T_m was found to be 55.5 ± 0.2 °C at 110 mM Na^+, supporting the conclusions from the CD studies that the RNA portion of the RNA−PEG conjugate forms a unimolecular hairpin.

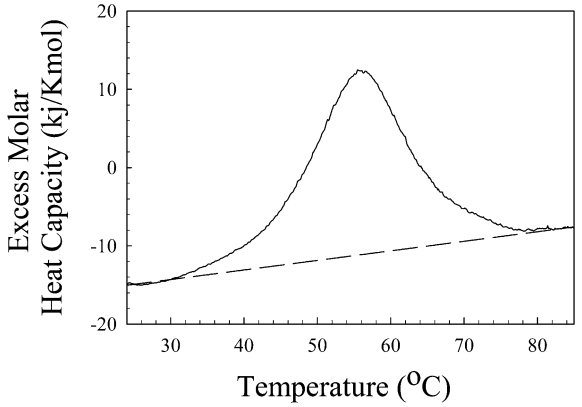

FIGURE 3: Typical DSC thermogram for the RNA (0.8 mg/mL) in standard phosphate buffer at 110 mM Na^+ at a heating rate of 0.5 °C/min. The solid line is the data, and the dashed line is the baseline.

Differential Scanning Calorimetry. The best approach for determining thermodynamic stability of nucleic acid duplexes is through the use of differential scanning calorimetry. Figure 3 shows a typical DSC thermogram for the RNA aptamer. The data are plotted as excess molar heat capacity vs temperature. After baseline correction, integration of the resultant peak gives $\Delta H_{cal} = 378.0 \pm 10$ kJ/mol with a T_m of 55.5 ± 0.2 °C, in excellent agreement with the optical melting derived enthalpy and T_m. Hence, the RNA aptamer hairpin is quite enthalpically stable under physiological conditions. The entropic contribution to the total free energy of duplex denaturation can be determined using the CpCalc software of the DSC, and this calculation gives $\Delta S = 1.15 \pm 0.1$ kJ/kmol. Using the Gibbs equation $\Delta G = \Delta H - T\Delta S$, one can determine the free energy of the transition at 37 °C (i.e., 310 K) to be +21.5 kJ/mol.

The ratio of the van't Hoff model-dependent enthalpy to the model-free calorimetric enthalpy can reveal information about the nature of the transition (*12*). Within the limits of the uncertainties of the determined values here, this ratio is essentially 1 (i.e., $\Delta H_{vH}/\Delta H_{cal} = 1.02$), indicative of a two-state transition. As noted above, the optical melting curve in Figure 2A suggested some deviation from two-state behavior. However, due to the agreement between the van't Hoff and calorimetric enthaplies, we conclude that any deviation from two-state behavior is minor.

Influence of Na^+ Concentration. RNA is a highly charged polyelectrolyte, and the phosphate groups strongly affect its structure and stability. As the salt concentration increases, intrastrand and interstrand phosphate−phosphate repulsions decrease, allowing for helix winding and, thus, better stacking of the base pairs. Figure 2C reveals that the T_M of the RNA aptamer increases linearly with ln [Na^+] in a fashion predicted by Record et al. (*7*).

Using the slope of the least-squares linear regression line, $\delta T_m/\delta$ ln [Na^+], the experimentally determined T_m, and ΔH values from above, one can calculate the differential ion binding term, Δn, using

$$\delta T_m/\delta \log [Na^+] = (RT_m^2/\Delta H)\Delta n$$

The differential ion binding term indicates the number of Na^+ released from the duplex into the bulk solution upon denaturation since single-stranded nucleic acids have lower charge densities than duplexes. The calculation indicates that

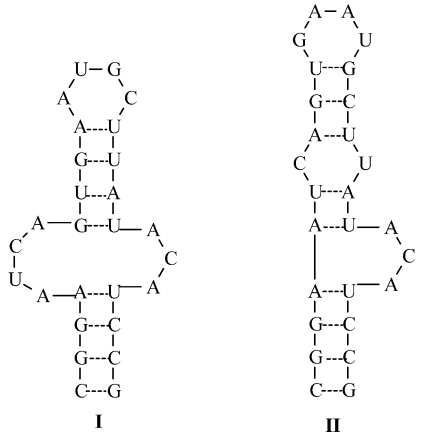

FIGURE 4: Proposed secondary structures for the RNA aptamer as generated by mfold (*3*, *15*). Structure **I** has a calculated folding free energy of −2.6 kcal/mol while structure **II** has a calculated free energy of folding of −3.0 kcal/mol (at 1 M Na^+). Structure **I** is identical to that proposed for a very similar sequence in ref *11*.

2.88 Na^+/RNA strand or 0.10 Na^+/phosphate are released from the hairpin upon thermal denaturation. For DNA duplexes, Δn is typically around 0.18 Na^+/phosphate at a solution concentration of Na^+ of 115 mM (*7*, *13*, *14*). Hence, we are observing less sodium ion loss from the RNA aptamer hairpin than for a normal DNA duplex. The difference is most likely due to the dramatically different secondary structure of the aptamer relative to a DNA duplex.

The CD and optical melting studies confirm that the secondary structure of the RNA is a hairpin with the stem assuming an A-like conformation. Inputting the sequence using unmodified bases into the RNA folding program mfold (*3*, *15*), two different structures of similar energetic stabilities were generated as shown in Figure 4. Structure **I** is in agreement with a previously reported structure for a similar sequence (*11*). It possesses three G·C base pairs, three A·U base pairs, two G·U base pairs, a four-base loop, and a three-base bulge opposite a four-base bulge with a calculated free energy of folding of −2.6 kcal/mol. On the other hand, structure **II** possesses four G·C base pairs, four A·U base pairs, only one G·U base pair, a four-base loop, a C-U bulge, and a three-base bulge with a calculated free energy of folding of −3.0 kcal/mol. Due to the slight difference in free energies between these two structures (400 cal/mol), it is likely that both structures would be present in solution for the unmodified RNA at 37 °C.

Both predicted values compare reasonably well for our experimentally determined value of −5.2 kcal/mol (i.e., −21.5 kJ/mol). The difference between the predicted values and the experimental values is due to several factors. First, the RNA used for this study is modifed at (1) the 5′ terminus with PEG, (2) the 3′ terminus with a 3′−3′ linkage to dT, and (3) the 2′ position of most of the bases; mfold allows for input of only unmodified bases. It is likely that these modifications influence the thermodynamic stability and hence the ultimate secondary structure of the RNA. Finally, the calculations in mfold are carried out at 1.0 M Na^+ whereas our experimentally values were determined at 110 mM Na^+.

The PEG modification is based solely on pharmacological reasons such as improved stability in the blood stream and improved delivery to the target tissue. PEG is an osmolyte

which could influence water activity and hence RNA stability. However, at the concentrations of RNA−PEG conjugate used for these studies, the influence of PEG as an osmolyte is negligible. Due to the unavailability of the unpegylated RNA, we were unable to evaluate the stability of the RNA without that modification.

To summarize, these studies indicate that the RNA portion of the RNA−PEG conjugate is a hairpin with assorted bulges and that the conformation of the duplexed region is A-like. Using an RNA folding program, two energetically similar but structurally different hairpins were generated. The various modifications of the RNA may influence the equilibrium between these two forms, and the actual solution conformation can only be resolved by high-resolution NMR studies which are beyond the scope of this work. If indeed there are two forms of the RNA in solution, they are indistinguishable thermodynamically since the denaturation is apparently two state. The thermodynamic data indicate that the secondary structure is quite stable under physiological conditions and its denaturation is highly reversible.

ACKNOWLEDGMENT

The authors thank the State of New Jersey Commission on Higher Education for a grant to purchase the differential scanning calorimeter.

REFERENCES

1. Mathews, D. H., and Turner, D. H. (2002) Dynalign: An Algorithm for Finding the Secondary Structure Common to Two RNA Sequences, *J. Mol. Biol. 317*, 191−203.
2. Burkard, M. E., Kierzek, R., and Turner, D. H. (1999) Thermodynamics of Unpaired Terminal Nucleotides on Short RNA Helixes Correlates with Stacking at Helix Termini in Large RNAs, *J. Mol. Biol. 290*, 967−982.
3. Mathews, D. H., Sabina, J., Zuker, M., and Turner, D. H. (1999) Expanded Sequence Dependence of Thermodynamic Parameters Improves Prediction of RNA, *J. Mol. Biol. 288*, 911−940.
4. Turner, D. H. (1996) Thermodynamics of Base Pairing, *Curr. Opin. Struct. Biol. 6*, 299−230.
5. Meroeh, M., and Chow, C. S. (1999) Thermodynamics of RNA Hairpins Containing Single Internal Mismatches, *Nucleic Acids Res. 27*, 1118−1125.
6. Wickstrom, E., and Tinoco, I., Jr. (1974) The Stability of RNA Hairpin Loops Containing A-U-G:A_n-U-G-U_m, *Biopolymers 13*, 2367−2383.
7. Record, M. T., Jr., Mazur, S. J., Melancon, P., Roe, J.-H., Shaner, S. L., and Unger, L. (1981) Double Helical DNA: Conformations, Physical Properties, and Interactions with Ligands, *Annu. Rev. Biochem. 30*, 997−1024.
8. Vogtherr, M., Schübel, H., and Limmer, S. (1998) Structural and Dynamic Geometry Alterations Induced by Mismatch Base Pairs in Double-Helical RNA, *FEBS Lett. 429*, 21−26.
9. Blackburn, G. M., and Gait, M. J. (1997) *Nucleic Acids in Chemistry and Biology*, 2nd ed., Oxford University Press, New York.
10. Ashkenas, J. (2004) APT Pupils: Nucleic Acid Drugs for Eye Disease, *Preclinica 2* (1), 10−12.
11. Ruckman, J., Greenm, L. S., Beeson, J., Waught, S., Gillette, W. L., Henninger, D. D., Claesson-Welsh, L., and Jancij, N. (1998) 2′-Fluoropyrimidine RNA-based Aptamers to the 165-Amino Acid Form of Vascular Endothelial Growth Factor ($VEGF_{165}$), *J. Biol. Chem. 273*, 20556−20567.
12. Marky, L. A., and Breslauer, K. J. (1987) Calculating Thermodynamic Data for Transitions of any Molecularity from Equilibrium Melting Curves, *Biopolymers 26*, 1601−1620.
13. Otokiti, E. O., and Sheardy, R. D. (1997) Sequence Effects on the Relative Thermodynamic Stabilities of B-Z Junction-Forming DNA Oligomeric Duplexes, *Biophys. J. 73*, 3135−3141.
14. Hicks, M., Wharton, G., III, Huchital, D. H., Murphy, W. R., Jr., and Sheardy, R. D. (1997) Assessing the Sequence Specificity in the Binding of Co(III) to DNA via a Thermodynamic Approach, *Biopolymers 36*, 549−559.
15. Zuker, M. (2003) Mfold Web Server for Nucleic Acid Folding and Hybridization Prediction, *Nucleic Acids Res. 31*, 3406−3415.

BI0521442